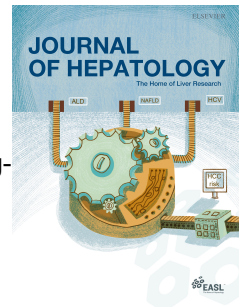

T-cell engager antibodies enable T cells to control HBV infection and to target HBsAg-positive hepatoma in mice

Oliver Quitt, Shanshan Luo, Marten Meyer, Zhe Xie, Forough Golsaz-Shirazi, Eva Loffredo-Verde, Julia Festag, Jan Hendrik Bockmann, Lili Zhao, Daniela Stadler, Wen-Min Chou, Raindy Tedjokusumo, Jochen Martin Wettengel, Chunkyu Ko, Elfriede Noeßner, Nadja Bulbuc, Fazel Shokri, Sandra Lüttgau, Mathias Heikenwälder, Felix Bohne, Gerhard Moldenhauer, Frank Momburg, Ulrike Protzer

PII: S0168-8278(21)00443-8

DOI: https://doi.org/10.1016/j.jhep.2021.06.022

Reference: JHEPAT 8329

To appear in: *Journal of Hepatology*

Received Date: 20 August 2020

Revised Date: 25 May 2021

Accepted Date: 2 June 2021

Please cite this article as: Quitt O, Luo S, Meyer M, Xie Z, Golsaz-Shirazi F, Loffredo-Verde E, Festag J, Bockmann JH, Zhao L, Stadler D, Chou WM, Tedjokusumo R, Wettengel JM, Ko C, Noeßner E, Bulbuc N, Shokri F, Lüttgau S, Heikenwälder M, Bohne F, Moldenhauer G, Momburg F, Protzer U, T-cell engager antibodies enable T cells to control HBV infection and to target HBsAg-positive hepatoma in mice, *Journal of Hepatology* (2021), doi: https://doi.org/10.1016/j.jhep.2021.06.022.

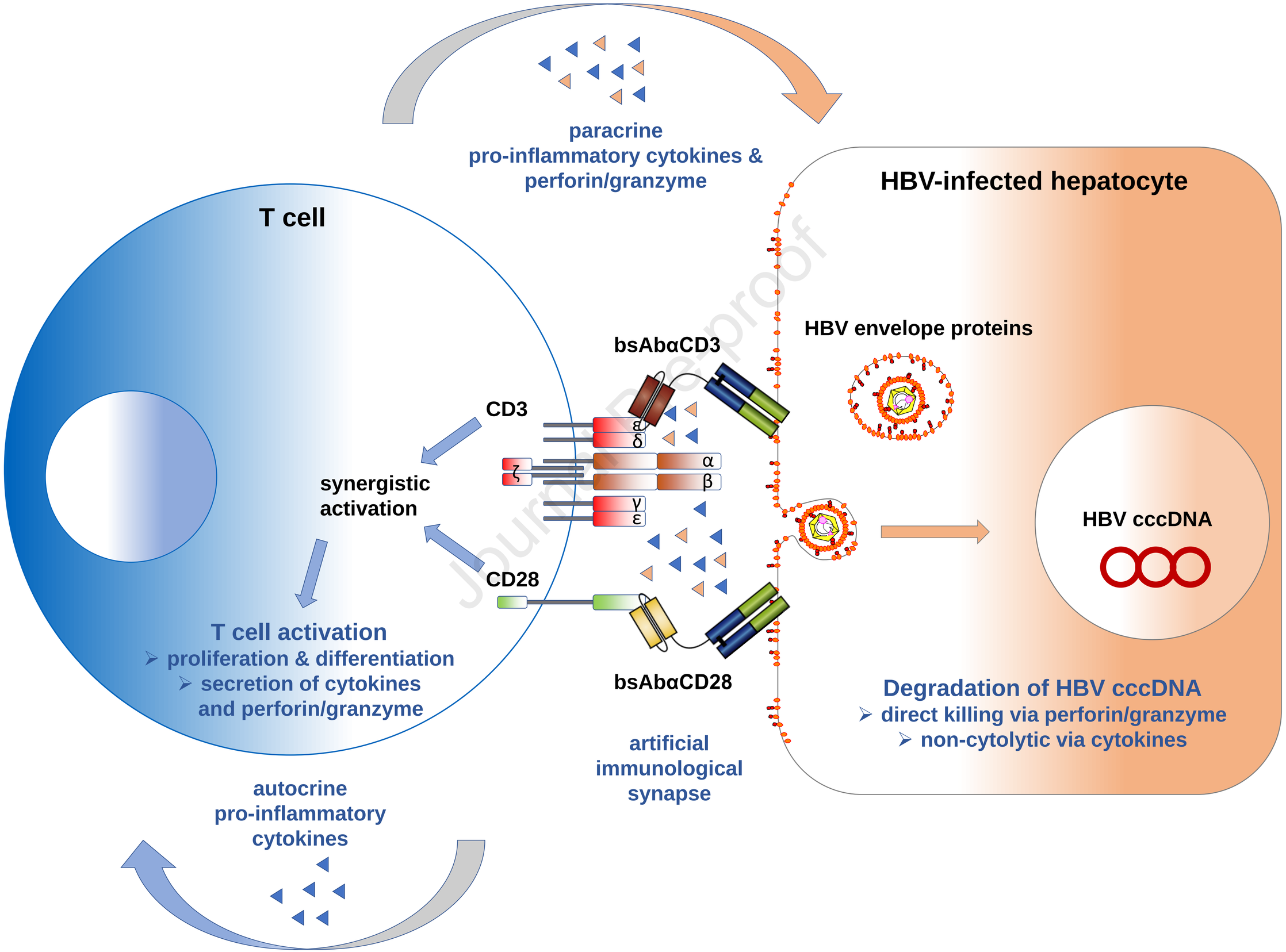
paracrine
pro-inflammatory cytokines &
perforin/granzyme
T cell
HBV-infected hepatocyte
HBV envelope proteins
bsAbαCD3
CD3
synergistic
activation
CD28
T cell activation
➢ proliferation & differentiation
➢ secretion of cytokines
and perforin/granzyme
bsAbαCD28
artificial
immunological
synapse
HBV cccDNA
Degradation of HBV cccDNA
➢ direct killing via perforin/granzyme
➢ non-cytolytic via cytokines
autocrine
pro-inflammatory
cytokines

T-cell engager antibodies enable T cells to control HBV infection and to target HBsAg-positive hepatoma in mice

Oliver Quitt[1#], Shanshan Luo[1,7#], Marten Meyer[2], Zhe Xie[1], Forough Golsaz-Shirazi[3], Eva Loffredo-Verde[1], Julia Festag[1], Jan Hendrik Bockmann[1,5,6], Lili Zhao[1], Daniela Stadler[1], Wen-Min Chou[1], Raindy Tedjokusumo[1], Jochen Martin Wettengel[1], Chunkyu Ko[1], Elfriede Noeßner[1], Nadja Bulbuc[2], Fazel Shokri[3], Sandra Lüttgau[4], Mathias Heikenwälder[1], Felix Bohne[1], Gerhard Moldenhauer[4], Frank Momburg[2], Ulrike Protzer[1,5,*]

[#] Both authors contributed equally to the work

[1]Institute of Virology, School of Medicine, Technical University of Munich / Helmholtz Zentrum München, Munich, Germany

[2]Antigen Presentation and T/NK Cell Activation Group, Clinical Cooperation Unit Applied Tumor Immunity, German Cancer Research Centre, Heidelberg, Germany

[3]Department of Immunology, School of Public Health, Tehran University of Medical Sciences, Tehran, Iran

[4]Department of Translational Immunology, German Cancer Research Centre, Heidelberg, Germany

[5]German Center for Infection Research (DZIF), Munich and Hamburg partner sites, Germany

[6]Department of Internal Medicine, University Medical Center Hamburg-Eppendorf, Hamburg, Germany

[7]Current address: Institute of Hematology, Union Hospital, Tongji Medical College, Huazhong University of Science and Technology, Wuhan, China

Short Titel: T-cell engager antibodies allow to target HBV

Corresponding author: Prof. Ulrike Protzer, MD; Institute of Virology, Technical University of Munich / Helmholtz Zentrum München; Trogerstr. 30, 81675 Munich, Germany; Tel: +49-89-4140-6886; Fax: -6823; e-mail: protzer@tum.de, protzer@helmholtz-muenchen.de.

Key words: Viral hepatitis, immunotherapy, bispecific T-cell engager, T-cell redirection

Electronic word count: 6637**; Numbers of figures and tables:** 8

Conflict of Interest Statement

U.P., F.M.,F.B., G.M. and O.Q. are named as inventors on patents WO 2015/036606 held by HMGU and DKFZ and WO 2016/146702 held by HMGU, DKFZ and TUM. U.P. serves as ad hoc advisor for Roche, Gilead, GSK, Merck, Arbutus and Vir Biotech. U.P. is co-founder and share-holder of SCG Cell Therapy who licensed patents WO 2015/036606 and WO 2016/146702. The remaining authors do not disclose a conflict of interest.

Financial support

The study was supported by the Helmholtz Association via the Helmholtz Validation Fund and the Deutsche Forschungsgemeinschaft (DFG) via TRR36 and TRR179 to MH and UP. JHB received a Clinician Scientist Stipend from the German Center for Infection Research (DZIF), Lili Zhao received a PhD stipend from the Chinese Scholarship Council and Wen-Min Chou received a stipend from the German Academic Exchange Service (DAAD).

Author Contributions

U.P., O.Q., S.L., F.M. and F.B. designed the study; O.Q., S.L., X.C., E.L.-V., C.K., J.F., R.T., W.-M.C., L.Z. and D.S. performed experiments; O.Q., S.L. and M.H., collected and analyzed data; E.N., M.M., N.B., F.G.S., F.S., S.L. and G.M. provided reagents; O.Q., S.L., F.M. and U.P. wrote the manuscript; J.H.B. and D.S. gave technical support and conceptual advice.

Abstract

Background & Aims: Hepatitis B virus (HBV) infection is a global health threat responsible for 880,000 deaths per year. Current antiviral therapies control but rarely eliminate the virus, and leave chronic HBV carriers at risk to develop hepatocellular carcinoma (HCC). Lacking or dysfunctional virus-specific adaptive immunity prevents control of HBV and allows the virus to persist. Restoring anti-viral T-cell immunity to achieve HBV elimination in chronically infected patients will help to cure HBV.

Methods: We constructed bispecific T-cell engager antibodies that are designed to induce anti-viral immunity through simultaneous binding of HBV envelope proteins (HBVenv) on infected hepatocytes and cluster of differentiation 3 or 28 on T cells. T-cell engager antibodies were employed in co-cultures with healthy donor lymphocytes and HBV-infected target cells. Activation of T-cell response was determined by detection of pro-inflammatory cytokines, effector function by cytotoxicity and antiviral effects. To study *in vivo* efficacy, immune-deficient mice were transplanted with HBV envelope-positive and -negative hepatoma cells.

Results: The two T-cell engager antibodies synergistically activated T cells to become polyfunctional effectors that in turn elicited potent anti-viral effects by killing infected cells and in addition controlled HBV via non-cytolytic, cytokine-mediated antiviral mechanisms. *In vivo* in mice, the antibodies attracted T cells specifically to the tumors expressing HBVenv resulting in T-cell activation, tumor infiltration and reduction of tumor burden.

Conclusion: This study demonstrates that the administration of HBVenv-targeting T-cell engager antibodies facilitates a robust T-cell redirection towards HBV-positive target cells and provides a feasible and promising approach for the treatment of chronic viral hepatitis and HBV-associated HCC.

Lay summary: T-cell engager antibodies are an interesting, novel therapeutic tool to restore immunity in patients with chronic hepatitis B. As bispecific antibodies they on the hand bind HBV envelope proteins displayed on the surface of HBV-infected cells or HBV-positive hepatoma and on the other hand attract and stimulate T cells by binding CD3 or CD28 on the T cell. Hereby, they activate a potent antiviral and cytotoxic response resulting in the elimination of HBV-positive cells. Their potential to activate T cells to resolve HBV infection renders T-cell engagers interesting candidates for the therapy of chronic hepatitis B and HBV-associated hepatocellular carcinoma.

Introduction

250 million humans worldwide are chronically infected with HBV often acquired around birth and at high risk to develop liver cirrhosis and HCC. Despite the availability of an effective prophylactic vaccine, morbidity as well as mortality of HBV infection have steadily increased over the last 20 years[1]. The infection often remains asymptomatic for years or even decades before inflammatory liver disease, chronic hepatitis B (CHB), or HCC develops[1]. Virus control is linked to CD4 and CD8 T-cell immunity but it is rare once the infection has become chronic[2].

Antiviral nucleos(t)ide analogues suppress viral replication by inhibiting reverse transcription, but do not target the persistence of HBV via its nuclear, covalently closed circular DNA (cccDNA) form. Interferon-α controls HBV infection in 5-15% of patients but has severe side effects. New therapeutic approaches are under evaluation[3] but so far none of those has proven to be curative. HBV cure, however, seems important to prevent integration of HBV and clonal expansion of hepatocytes and finally HCC that in 30-50% of cases develops even in the absence of liver cirrhosis[4].

To achieve HBV cure and to eliminate cells carrying HBV integrates, activation of HBV-specific immunity is required[5]. The concept of T cells as key players in the establishment of functional cure has inspired the development of immunotherapeutic approaches that aim to enhance or restore an HBV-specific T-cell response in CHB patients[5]. Therapeutic vaccines or checkpoint inhibitors may reactivate dysfunctional HBV-specific T cell responses. Alternatively, T cells can be engineered with HBV-specific T-cell[6] or a chimeric antigen receptors[7] enabling them to control and even eliminate HBV infection in humanized mice[8]. Production of such T cells, however, requires manipulation of cells in specific facilities. Therefore, bispecific antibodies (bsAbs) that can simply be injected and engage and redirect T cells to HBV infected

cells in the liver would be an interesting and more broadly applicable therapeutic alternative. Such T-cell engager antibodies have been developed for cancer immunotherapy showing clinical efficacy in B-cell malignancies, such as non-Hodgkin's lymphoma[9] or acute lymphoblastic leukemia[10], but may also serve as treatment option for infectious diseases[11, 12].

Here, we report the engineering of T-cell engager antibodies that target HBVenv on the surface of infected cells, and recruit and activate T cells by binding the T-cell receptor through CD3 and co-stimulatory CD28. We demonstrate that these T-cell engager antibodies are capable of specifically redirecting T cells towards HBV-infected cells, resulting in T-cell activation, inhibition of virus replication, killing of HBV-positive cells and control of HBVenv-expressing tumors *in vivo*.

Material and Methods (for details see supplementary information).

Cloning and production of HBV-specific bsAbs. HBV-binders recognizing the a-determinant contained in all three HBVenv proteins were single chain variable fragment (scFv) C8[7] and the Fab-fragment of monoclonal antibody 5F9[13]. BiMAb (Fig. 1Ai) represents a ~170 kD homodimer of two copies of HBVenv-specific scFv C8[7] connected via a $(G_4S)_3$ linker to the N-termini of a modified IgG1 Fc domain containing mutations C220S, E233P, L234A, L235A, G236del, N297Q, K322A, A327G, P329A, A330S, and P331S. CD3-specific scFv generated from variable domains of OKT3[14], or a CD28-specific scFv derived from antibody 9.3[15] was linked C-terminally. FabMAb (Fig. 1Aii) is a ~78 kD bivalent binder composed of the human IgG-CH1 and scFv from antibody 5F9[13] connected to the CD3- or CD28-specific scFvs by a glycine-serine $(G_4S)_3$ linker. FabMAb were equipped with a C-terminal His-tag and BiMAb with a Strep-tag II between the Fc domain and the C-terminal scFvs, and expressed in HEK293 cells. BiMAb were purified via protein A and size exclusion chromatography by Proteros Biostructures (Martinsried, Germany), FabMAb using metal chelate affinity size exclusion chromatography by InVivo Biotech Services (Henningsdorf/Berlin, Germany).

Binding analysis of bsAbs to HBVenv. For enzyme-linked immunosorbent assay (ELISA), 1 µg/ml HBsAg purified from patient serum was coated (kindly provided by Roche Diagnostics, Penzberg, Germany). A dilution series of bsAb (half-logarithmic 1000-0.003 nM) was added. Bound antibodies were detected using goat anti human IgG antibodies (Sigma Aldrich), anti-6x His-Tag antibody HRP-conjugate (Invitrogen, Karlsruhe, Germany) or StrepMAb classic-HRP (Iba Lifescience, Göttingen, Germany), respectively. A genotype panel of HBsAg (Paul-Ehrlich-Institut, Langen, Germany) was captured with HBVenv-specific antibodies (Murex HBsAg

Version 3, DiaSorin, Saluggia, Italy) and detected using 50 nM FabMAb or 100 nM BiMAb.

$0.7x10^6$ Huh7 cells were transfected with 5 µg mCherry-S fusion plasmid DNA and stained with 50 nM of bsAbs, Alexa Fluor 647 goat anti-human IgG (ThermoFisher), and Alexa 488 coupled wheat germ agglutinine (ThermoFisher) before fixation and analysis by confocal microscopy.

Binding of bsAbs to peripheral blood mononuclear cells (PBMC) subsets. Human PBMC were isolated and incubated with 10 nM BiMAbαCD3, 300 nM BiMAbαCD28, 30 nM FabMAbαCD3, and 3 µM FabMAbαCD28 and stained using LIVE/DEAD™ Kit (NIR, ThermoFisher) as well as anti-CD8 PB (BioLegend, San Diego, USA) anti-CD4 APC (Invitrogen) for T cells, anti-CD19 ef450 (ebioscience, Frankfurt, Germany) for B-cells, anti-CD3 FITC (Invitrogen) and anti-CD56 APC (Beckman Coulter, Brea, USA) for NK cells, anti-CD3 AF700 (BD Biosciences, Heidelberg, Germany) and anti-CD14 BV421 (BD) for monocytes. BiMAb and FabMAb were stained with anti-human IgG Fc PE (BioLegend) and anti-His Tag PE (BioLegend), respectively. Cells were analyzed using a Cytoflex S (Beckman Coulter). T-cell depletion and isolation was performed using the human $CD4^+$ T cell and $CD8^+$ T cell isolation kit (Myltenyi Biotec, Bergisch Gladbach, Germany) according to the manufacturers protocol.

Assessment of T-cell activation. PBMC and bsAbs were added to 96-well cell culture plates coated with either 5 µg/ml HBsAg or PBS, or to HuH7 or Huh7S cells (stably expressing HBV S, genotype A), or to HepG2 or HepG2 660 cells (stably expressing HBV SML, genotype D). Supernatants were collected after 72 hours and analyzed by ELISA for cytokines interferon-gamma (IFNγ), tumor necrosis factor alpha (TNFα) and interleukin-2 (IL-2) or using Bio-Plex human Cytokine Group I Panel 17-Plex (Luminex Corp, Austin, TX, USA). Flow cytometry was used to

identify T-cell phenotypic and activation markers and intracellular cytokines and to determine T cell proliferation. Cytotoxicity was assessed in 96-well E-plates for 96 hours employing an xCELLigence real-time cell analyzer SP device (ACEA Biosciences, San Diego, USA).

Antiviral effect on HBV-infected cells. HepG2-NTCP K7 cells[16] were seeded in 6-well or 24-well cell culture plates, differentiated and infected with HBV purified for supernatant of HepAd38 cells[16]. 8-10 days post infection, PBMC were added and bsAbs were supplied every two days for 12 days. For xCELLigence experiments, infected cells were transferred to 96-well E-plates. Secreted hepatitis B surface (HBsAg) and e antigen (HBeAg) were quantified using the Architect™ platform (Abbott Laboratories, Abbott Park, IL, USA), and intracellular total HBV-DNA and HBV cccDNA were quantified by qPCR and Southern blot as described before[16, 17] (primer sequences in CTAT table). Intracellular HBVcore staining was analyzed by flow cytometry[18].

To study non-cytolytic antiviral effects, PBMC were cultured in Corning polyester transwell inserts (Corning, New York, USA) with 0.4 µm pore size (Sigma) and activated on Huh7S cells in the presence or absence of BiMAb for 24 hours. Inlets were transferred to 12-well cell cultures, in which differentiated HepaRG cells infected with HBV (MOI 100) were cultured[17]. After 7 days, pro-inflammatory cytokines and viral parameters in the supernatant, as well as intracellular HBV-DNA were quantified.

Animal experiments. Rag2/IL2Rγc$^{-/-}$ mice (Balb/c background), HBVtg HBV1.3xfs mice (HBVQ9 genotype D, serotype ayw13, C57BL/6 background) and C57BL/6 mice were kept in a specific-pathogen-free (SPF) facility under appropriate biosafety conditions and received humane care. Animal experiments were conducted in strict accordance to the German regulations of the Society for Laboratory Animal Science

and the European Health Law of the Federation of Laboratory Animal Science Associations. Experiments were approved by the local Animal Care and Use Committee of Upper Bavaria (permission number: 55.2-1-54-2532-57-14) and followed the 3R rules.

Evaluation of bsAbs *in vivo*.

To follow liver targeting, 50 or 100 µg of BiMAb were intravenously injected into HBV1.3xfs or C57BL/6 control mice. 2 hours after injection, livers were fixed and stained with either Hematoxylin-Eosin (HE) or, for detection of bsAbs, with HRP-coupled goat-anti-human antiserum. Positive cells were quantified from at least three tissue areas adding up to ≥10 mm^2.

To determine pharmacokinetics, three C57BL/6 mice per group were injected intravenously (i.v.), intraperitoneally (i.p.) or subcutaneously (s.c.) with 50 µg of BiMAbαCD3 or FabMAbαCD28. Control mice received PBS i.v. Serum FabMAb concentrations were detected by goat anti-human Fab HRP antibodies (Sigma-Aldrich/Merck) by ELISA. BiMAb concentrations were quantified using the Architect™ anti-HBs assay (Abott Laboratories).

To determine the anti-tumor effect, 28 age- and gender-matched Rag2/IL2Ryc$^{-/-}$ mice were injected subcutaneously with 2x10^6 HuH7 cells into the left and 2x10^6 HuH7S cells into the right flank. Freshly isolated PBMC were CD3/CD28-stimulated and expanded with IL-2. After 14 days, when tumors were established, 2x10^7 PBMC were injected i.p. and a combination of BiMAbαCD3 and BiMAbαCD28 (100 µg/mouse) or PBS i.v. on day 14, 16, 18 and 20. Tumour size was measured using a calliper and all visible tumour tissue was collected for mRNA isolation and qPCR of human $CD4^+$, $CD8^+$, TNFα, IFNγ and IL-2. Serum was collected to quantify HBsAg levels.

Statistical analyses. Statistical analyses were performed with Prism 5.01.336 (Graphpad). Data sets were analyzed for Gaussian distribution with D'Agostion-

Pearson omnibus test. Depending on the result parametric student t-test or non-parametric Mann-Whitney test was employed. P-values <0.05 were considered significant. EC_{50} was calculated using non-linear regression log(agonist), IC_{50} with non-linear regression log(inhibitor) vs. normalized response variable slope with a robust fit.

Results

BiMAb and FabMAb specifically interact with their target proteins

We developed two structurally different bsAb formats: BiMAb and FabMAb (Fig.1A). Polyacrylamide gel electrophoresis (Fig.1B, Supplementary Fig.1A) confirmed expected molecular weights of BiMAb homodimers (~85 kD under reducing conditions), and FabMAb heterodimers (~55 and ~23 kD, respectively) corresponding to heavy chain scFvCD3/CD28- and light chain polypeptides.

Flow cytometry confirmed binding of all four bsAbs specifically to $CD4^+$ and $CD8^+$ T cells (Fig.1C,D). Hereby, CD3-targeting bsAbs showed a higher affinity than CD28-targeting bsAbs (Supplementary Fig.1B). To exclude bsAb binding to NK cells, B cells and monocytes, we stained $CD3^-$ PBMC for CD19, CD56 as well as CD14 (Supplementary Fig.1C) but detected no positive signal (Fig.1C,D).

EC_{50} for binding to HBsAg determined by ELISA was <2.5 nM for all constructs with C8 scFv used in BiMAb showing a slightly higher affinity than the 5F9 Fab-fragment employed in the FabMAb constructs (Fig.2A). HBVenv antibodies C8 and 5F9 were able to bind all known HBV geno- and subtypes though with different affinity (Fig.2B). Confocal microscopy revealed binding of bsAbs to HBVenv on the hepatocyte cell membrane with positive staining exclusively found on mCherry-HBVenv transfected cells (Fig.2C). From these data, we concluded that our BiMAb and FabMAb constructs serve as T-cell engagers binding HBVenv on the surface of hepatoma cells and CD3 or CD28 on T cells, and are applicable for a broad range of HBV variants.

BiMAb and FabMAb serve as T-cell engagers and induce polyfunctional effector T cells

When freshly isolated PBMC from healthy subjects were cultured on plates coated with HBsAg in the presence of bsAbs, T cells were activated and upregulated CD25 (Fig.3A,B), translocated lysosomal associated membrane protein 1 (LAMP-1) (Fig.3B, Supplementary Fig.2A-D), and started to proliferate (Fig.3C) and secreted IFNγ, IL-2 and TNFα (Fig.3D, Supplementary Fig.3A,B). Single bsAbs only resulted in low-level T-cell activation but the combination of CD3- and CD28-binding bsAbs clearly showed a synergistic effect (Fig.3A-C).Therefore, a combination of CD3- and CD28 binders was used in further experiments.

When PBMC were co-cultured with HBVenv-expressing Huh7 (Huh7S) cells and either BiMAb or FabMAb were added, secretion of IFNγ, IL-2 and TNFα indicating polyfunctional T-cell activation started after 8 and increased until 72 hours (Fig.3E, Supplementary Fig.4A,B,C). By intracellular cytokine staining, first cytokine expression was detected after 4 hours, and after 48 hours, ~50% of $CD8^+$ and $CD4^+$ T cells stained positive for at least one of the cytokines (Fig.2F, Supplementary Fig.5A,B and 6A,B). In depth analysis employing the Luminex technology detected the secretion of a panel of cytokines, especially IL-1beta, IL-10, IL-13 and Rantes (Fig.3G, Supplementary Fig.7). In controls containing either no bsAbs or no antigen, ~50% of T cells remained naive, ~10% each were classified effector-memory and effector memory re-expressing CD45RA, and 30% were classified central memory T cells[19]. In antibody-treated samples in contrast, >80% of T cells showed a memory phenotype, while the percentage of naïve T cells was substantially reduced (Fig.3H; Supplementary Fig.8A,B). These data indicate that our T-cell engagers are able to redirect T cells towards Huh7S cells, resulting in proliferation and polyfunctional activation of $CD4^+$ and $CD8^+$ T cells.

T-cell engager antibodies activate cytotoxic T-cell function

More than 90% of $CD4^+$ and $CD8^+$ T cells stained positive for intracellular granzyme B 48 hours after addition of bsAb (Fig.4A, Supplementary Fig.9A,B). Viability of HuH7S cells decreased starting within hours. BsAb concentrations of ≥1 nM resulted in complete killing of targets within 96 hours (Fig.4B), while we detected no or only a minor loss of HBV-negative Huh7 control cells (Supplementary Fig.10A,B).

Individual depletion of either $CD4^+$ or $CD8^+$ T cells from PBMC (Supplementary Fig.11) had no or only a minor effect on killing kinetics, respectively, while depletion of both, $CD4^+$ and $CD8^+$ T cells, prevented cytotoxicity (Fig.4C). Along this line, purified $CD4^+$ and $CD8^+$ T-cells were able to effectively kill Huh7S target cells, whether applied singly or in combination (Fig.4D). Efficient IFNγ secretion, however, required the presence of $CD4^+$ T cells (Fig. 4E). When using PBMC from an CHB patient, the killing kinetics were comparable to that observed with PBMC of four different healthy donors (Fig.4F).

To study the specificity of T-cell redirection, we mixed HepG2 cells with 25, 50, 75 or 100% of HBVenv-transgenic HepG2 660 cells, and cultured them with PBMC and bsAbs. The loss of cell viability correlated with the percentage of HBVenv-positive cells (Fig.4G). IFNγ levels in the supernatant correlated well with the percentage of HBVenv-positive target cells, with an R squared of 0.9 for both bsAb formats (Fig.4H). This excluded a significant stimulating effect of soluble HBsAg released from Huh7S cells that may have resulted in bystander killing of neighboring Huh7 cells after adsorption.

Taken together, these data show that T-cell engager antibodies license both, $CD4^+$ and $CD8^+$ T-cells to kill target cells in the presence of antigen, and activate T cells from healthy donors as well as CHB patients to specifically kill HBVenv-expressing target cells.

T-cell engagers activate T cells to eliminate HBV-infected hepatocytes

To analyze if our T-cell engager antibodies were able to target HBVenv on the surface of HBV-infected cells, we infected HepG2-NTCP cells[16] using a multiplicity of infection (MOI) of 500 HBV virions/cell. By flow cytometry analysis of infected cells stained for HBV core, we determined the percentage of infected HepG2-NTCP cells to be around 60% (Fig.5A) and confirmed binding of BiMAb to these cells (Fig.5B). To study the correlation between the level of infection and the efficacy of T-cell redirection, we infected HepG2-NTCP cells with different amounts of HBV and co-cultured them with PBMC in presence of a serial dilution of FabMAb. IFNγ, IL-2 and TNFα secreted from activated T cells increased with the antibody concentration and the MOI used (Fig.5C). BiMAb as well as FabMAb induced killing of infected target cells in a dose-dependent fashion, while infected control cells cultured with PBMC in the absence of bsAbs, and non-infected controls in the presence of PBMC and BiMAb or FabMAb remained viable (Fig.5D). The percentage of target cells killed was around 60% and correlated well with the amount of infected cells determined by HBV core-staining indicating specific elimination of HBV-infected cells.

T-cell engager antibodies stimulate antiviral activity of T cells

To analyze the antiviral potency of T cells activated by our bsAbs, we assessed the levels of viral antigen secreted from HBV-infected cells and the levels of intracellular HBV DNA. HBeAg levels were reduced by >90% at 1 nM or 10 nM FabMAb and up to 70% at 10 nM BiMAb (Fig.6A). This correlated strongly with the reduction of intracellular HBV genomic (rc)DNA and cccDNA detected by Southern blot analysis (Fig.6B) and qPCR (Fig.6C). Non-linear regression analysis of the viral markers determined that BiMAb and FabMAb inhibit HBV at inhibitory concentrations $(IC)_{50}$ of

2.25-2.43 nM and 0.25-0.40 nM, respectively. As the analyses were done using HBV genotype D, the higher efficacy of FabMAb can be explained by the higher binding affinity of the 5F9 binding domain to genotype D HBsAg (Fig.2B).

Next, we infected HepG2-NTCP cells with increasing amounts of HBV and treated them with FabMAb. In HepG2-NTCP cells infected with HBV at MOI >50 virions/cell, HBV markers were significantly reduced at 1 and 10 nM concentrations with HBeAg being up to 90% and intracellular HBV-DNA and cccDNA >99% reduced at highest MOIs (Fig.6E).

Since antiviral cytokines can control HBV and the viral persistence form, cccDNA, can be specifically degraded by non-hepatotoxic mechanisms[17, 20], we asked whether T-cell engagers activate cytokine-mediated antiviral effects. We cultured PBMC, Huh7S cells and BiMAb or FabMAb in a transwell system that allowed for diffusion of T-cell cytokines to HBV-infected HepaRG cells but prevented direct killing of the infected hepatoma cells[17]. A significant reduction of HBeAg, intracellular HBV-DNA and cccDNA in HBV-infected HepaRG cells without direct contact to activated T cells demonstrated a strong cytokine-mediated antiviral effect. The antiviral effect correlated directly with the levels of IFNγ, IL-2 and TNFα secreted (Fig.6F, Supplementary Fig.12A-C). We therefore concluded that our T-cell engagers are capable to redirect T cells towards HBV-infected cells and activate them to control HBV by killing infected cells, but also by cytokine-mediated, non-cytolytic antiviral activity.

BiMAb target HBVenv-expressing hepatocytes *in vivo*

To study the T-cell redirection capacity of bsAbs *in vivo*, we injected C57BL/6 mice intravenously (i.v.), intraperitoneally (i.p.), or subcutaneously (s.c.) with 50 µg of BiMAbαCD28 or FabMAbαCD28 and determined serum antibody levels. Similar

kinetics were observed after i.v. or i.p. administration for both antibody formats. FabMAb serum levels dropped rapidly with a half-life ($t_{1/2}$) <6 hours, while BiMAb persisted longer reaching a plateau at around 50% of the initial input after 48 hours, resulting in a $t_{1/2}$ of >72 hours (Fig.7A,B). After s.c. injection, FabMAb was hardly detectable, while BiMAb levels increased continuously within the first 48 hours reaching the same level as the other routes (Fig.7A,B). Due to the substantially longer half-life, we selected BiMAb for further *in vivo* experiments.

To assess if BiMAb are able to reach the liver and target the HBVenv on the hepatocyte membrane, we i.v. injected 50 µg and 100 µg of BiMAbαCD3 or BiMAbαCD28 into HBV1.3xfs transgenic and HBV-naïve C57BL/6 control mice (Fig.7C,D) and analyzed livers two hours after injection. Livers of BiMAb-treated HBV1.3xfs mice stained positive for human IgG along the hepatic sinusoids, while livers of PBS-injected as well as C57BL/6 control animals were negative (Fig.7C,D). This demonstrated that BiMAb reach the liver within the first two hours after systemic application and target HBV-replicating hepatocytes.

BiMAb control HBVenv-expressing tumors *in vivo*

Because patients with advanced, HBVenv-positive HCC will probably be the first to benefit from this novel therapeutic approach, we decided to test BiMAb *in vivo* in a tumor model. Since our bsAbs can only bind human T cells, we injected human hepatoma cells into immune-deficient $Rag2^{-/-}$/$IL2Ryc^{-/-}$ mice. 28 mice were injected subcutaneously with $2x10^6$ Huh7 or Huh7S cells into the left and the right flank, respectively. After 14 days, mice were intraperitoneally injected with $2x10^7$ human PBMC and i.v. injected with either 100 µg of a BiMAbαCD3/CD28 combination (corresponding to ~2.5 mg/kg body weight) or PBS. Antibody injections were

repeated three times every two days. After ten days of treatment, mice were sacrificed and tumors as well as sera were collected (Fig.8A).

While the size of HBVenv-negative tumors was comparable between both groups, HBVenv-positive tumors were significantly smaller in BiMAb-treated animals (Fig.8B). To estimate the amount of tumor-infiltrating lymphocytes, we determined the presence of human CD4, CD8 and cytokine transcripts via qPCR in all visible tumors. A significant increase of CD8 mRNA in BiMAb-treated mice indicated an infiltration of human T cells into HBVenv expressing (Fig.8C), but not into HBVenv negative tumors (Fig. 8D). While in mice that were tumor free T cell infiltration could not be studied anymore, we detected higher levels of $CD4^+$ and $CD8^+$ mRNA in those mice that had a reduced tumor size. In addition, mRNA levels of IFNγ, and in tendency IL-2 and TNFα, were increased in tumors of BiMAb-treated mice (Supplementary Fig.13). HBsAg serum levels in the BiMAb-treated group were significantly reduced (Fig.8E). These data indicate that BiMAb can redirect T cells towards HBVenv-expressing tumors *in vivo*, resulting in T-cell infiltration of HBVenv-positive tumors, T-cell activation and specific killing of tumor cells.

Discussion

A current goal of many activities in academia, biotech and pharmaceutical industry is to develop a curative treatment for CHB to prevent HCC development[3]. Here, we describe the successful engineering of novel, bispecific T-cell engager antibodies that target T cells to HBV-infected cells and to hepatoma cells that express HBVenv from integrated DNA. Our T-cell engager antibodies establish and maintain a specific and polyfunctional T-cell response in cell culture and attract T cells *in vivo* specifically into HBVenv-expressing tumors. When activated by our T-cell engagers, T cells show cytolytic and non-cytolytic, antiviral activity to diminish the burden of HBV-

infection. Thus, T cells were able to control HBV replication and eliminate HBV-infected cells as well as HBV-positive hepatoma *in vivo*, and provide a promising approach for the treatment of CHB and HBV-associated HCC.

We designed two different antibody formats to target HBsAg-positive cells employing identical T-cell binding scFv but different HBVenv binders yet with similar binding affinity[7, 13]. They recognize a conformational epitope within the small (S) envelope protein that can be targeted by chimeric antigen receptors[7] on the surface of HBV-replicating cells. HBVenv is also expressed by integrated HBV-DNA in CHB[21] and by a significant number of HBV-associated HCC. In particular the C8 scFv included in our BiMAb targets all major HBV genotypes A to F that make up for >96% of the HBV strains found worldwide including those in South America and Africa[22] allowing broad application.

BiMAb are tetravalent antibodies providing two binding domains for HBVenv and CD3/CD28 while FabMAb are bivalent providing one of each. Both, however, induced comparable T-cell proliferation, cytokine expression and killing of transgenic target cells that express HBVenv of genotype A. In infection experiments with HBV genotype D, FabMAb showing higher binding affinity to this genotype was even a little more potent. This demonstrates that affinity of the binder to the target antigen largely influences the efficacy of a T-cell engager.

Regarding serum half-life *in vivo*, the smaller FabMAb only had a $t_{1/2}$ below 6 hours in line with BiTEs of similar size[23] and require continuous infusion for therapy. BiMAb, with a molecular weight that limits renal elimination and allows recycling through the neonatal Fc receptor, had a $t_{1/2}$ of >72 hours and were therefore used in a tumor transplant model that demonstrated the functionality of our T-cell engager antibodies *in vivo*. I.v. injected BiMAb engaged i.p. administered T cells and redirected them

specifically to HBVenv-positive tumors, resulting in T-cell activation, tumor infiltration and control of tumor growth. Circulating HBsAg did not prevent tumor targeting.

Our T-cell engager antibodies bound specifically to T cells with a slightly higher affinity for $CD4^+$ T cells activating polyfunctional T-cell responses with profound secretion of IFNγ and TNFα. We confirmed that these cytokines can induce cccDNA degradation and control HBV in a non-cytolytic fashion[17, 20]

Potent T-cell activation required CD28 co-stimulation in our setting. CD3-specific bsAbs are sufficient to induce efficient lymphoma cell killing in cancer immunotherapy. A recent study targeting CD38 on myeloma, clearly demonstrated superiority of simultaneous stimulation of CD3 and CD28 by T-cell engagers *in vivo*. Similar to our study, stimulation of CD3 and CD28 suppressed tumor growth in a humanized mouse model, stimulated memory/effector T-cell proliferation and also reduced regulatory T cells in non-human primates at well-tolerated doses[24]. These findings argue that co-stimulation via CD28 can be beneficial in the setting of antibody mediated T-cell redirection, although potential side effects certainly need to be carefully evaluated. We expect HBVenv to be exposed at the cell surface at relatively low levels, requiring a co-stimulatory signal that increases T-cell sensitivity[25]. Isolated $CD4^+$ T cells displayed comparable bsAb-mediated cytotoxicity activity as $CD8^+$ T cells, which has been described for BiTE-stimulated T cells from PBMC[26].

Potential bystander killing is an important concern when translating an immunotherapy into the clinics. We here demonstrate specific, T-cell mediated elimination of target cells with three different HBVenv-expressing cells lines. *In vivo,* no effect on HBVenv-negative tumor cell growth was observed. This strongly argues against unwanted bystander killing. However, in our experimental setting there is an MHC miss-match between donor PBMC and target cells that may trigger

cytotoxicity enhanced by low-level CD3 and CD28 engagement. Such an MHC miss-match, however, will not be an issue when a patient's endogenous T cells become activated.

Taken together, this study demonstrates that the administration of HBVenv-targeting, bispecific T-cell engager antibodies facilitates robust and specific T-cell redirection towards HBV-positive target cells and provides a feasible and promising approach for the treatment of CHB and HBV-associated HCC.

Abbreviations

bsAbs, bispecific T-cell engager antibodies; cccDNA, covalently closed circular DNA; CHB, chronic hepatitis B; Fab, fragment antigen-binding; grzB, granzyme B; HBVenv, hepatitis B virus envelope protein; Huh7S, HBVenv-expressing Huh7; IFNγ, interferon-γ; IL-2, interleukin-2; LAMP-1, lysosomal-associated membrane protein; MOI, multiplicity of infection; PBMC, peripheral blood mononuclear cells; S, small HBV envelope protein; scFv, single-chain variable fragment; TNFα, tumor necrosis factor;

Acknowledgements

The authors thank Theresa Asen, Romina Bester and Philip Hagen for excellent technical support. The work was supported by funds from the German Research Foundation (DFG) via TRR179, project No. 272983813/TP14 to UP, via the Helmholtz Validation Fund to UP and FM, via the Helmholtz-Aberta-Initiative (HAI-IDR) and by Hoffmann-La Roche Ltd via Research Agreement 2016191. We thank Siemens Healthcare/Diasorin for supporting HBeAg diagnostics.

References (Author names in bold designate shared co-first authorship)

1. Thomas DL. Global Elimination of Chronic Hepatitis. N Engl J Med 2019;380:2041-2050.
2. Protzer U, Maini MK, Knolle PA. Living in the liver: hepatic infections. Nat Rev Immunol 2012;12:201-213.
3. Fanning GC, Zoulim F, Hou J, Bertoletti A. Therapeutic strategies for hepatitis B virus infection: towards a cure. Nat Rev Drug Discov 2019;18:827-844.
4. Yang JD, Hainaut P, Gores GJ, Amadou A, Plymoth A, Roberts LR. A global view of hepatocellular carcinoma: trends, risk, prevention and management. Nat Rev Gastroenterol Hepatol 2019;16:589-604.
5. Gehring AJ, Protzer U. Targeting Innate and Adaptive Immune Responses to Cure Chronic HBV Infection. Gastroenterology 2019;156:325-337.
6. Qasim W, Brunetto M, Gehring AJ, Xue SA, Schurich A, Khakpoor A, et al. Immunotherapy of HCC metastases with autologous T cell receptor redirected T cells, targeting HBsAg in a liver transplant patient. J Hepatol 2015;62:486-491.
7. Bohne F, Chmielewski M, Ebert G, Wiegmann K, Kurschner T, Schulze A, et al. T cells redirected against hepatitis B virus surface proteins eliminate infected hepatocytes. Gastroenterology 2008;134:239-247.
8. Wisskirchen K, Kah J, Malo A, Asen T, Volz T, Allweiss L, et al. T cell receptor grafting allows virological control of hepatitis B virus infection. The Journal of Clinical Investigation 2019;129:2932-2945.
9. Bargou R, Leo E, Zugmaier G, Klinger M, Goebeler M, Knop S, et al. Tumor regression in cancer patients by very low doses of a T cell-engaging antibody. Science 2008;321:974-977.
10. Hoffman LM, Gore L. Blinatumomab, a Bi-Specific Anti-CD19/CD3 BiTE((R)) Antibody for the Treatment of Acute Lymphoblastic Leukemia: Perspectives and Current Pediatric Applications. Front Oncol 2014;4:63.

11. Sloan DD, Lam CY, Irrinki A, Liu L, Tsai A, Pace CS, et al. Targeting HIV Reservoir in Infected CD4 T Cells by Dual-Affinity Re-targeting Molecules (DARTs) that Bind HIV Envelope and Recruit Cytotoxic T Cells. PLoS Pathog 2015;11:e1005233.
12. Kruse RL, Shum T, Legras X, Barzi M, Pankowicz FP, Gottschalk S, et al. In Situ Liver Expression of HBsAg/CD3-Bispecific Antibodies for HBV Immunotherapy. Mol Ther Methods Clin Dev 2017;7:32-41.
13. Golsaz-Shirazi F, Mohammadi H, Amiri MM, Khoshnoodi J, Kardar GA, Jeddi-Tehrani M, et al. Localization of immunodominant epitopes within the "a" determinant of hepatitis B surface antigen using monoclonal antibodies. Arch Virol 2016;161:2765-2772.
14. Kung P, Goldstein G, Reinherz EL, Schlossman SF. Monoclonal antibodies defining distinctive human T cell surface antigens. Science 1979;206:347-349.
15. Baroja ML, Lorre K, Van Vaeck F, Ceuppens JL. The anti-T cell monoclonal antibody 9.3 (anti-CD28) provides a helper signal and bypasses the need for accessory cells in T cell activation with immobilized anti-CD3 and mitogens. Cell Immunol 1989;120:205-217.
16. Ko C, Chakraborty A, Chou WM, Hasreiter J, Wettengel JM, Stadler D, et al. Hepatitis B virus genome recycling and de novo secondary infection events maintain stable cccDNA levels. J Hepatol 2018;69:1231-1241.
17. **Xia Y, Stadler D**, Lucifora J, Reisinger F, Webb D, Hosel M, et al. Interferon-gamma and Tumor Necrosis Factor-alpha Produced by T Cells Reduce the HBV Persistence Form, cccDNA, Without Cytolysis. Gastroenterology 2016;150:194-205.
18. Ko C, Bester R, Zhou X, Xu Z, Blossey C, Sacherl J, et al. A New Role for Capsid Assembly Modulators To Target Mature Hepatitis B Virus Capsids and Prevent Virus Infection. Antimicrob Agents Chemother 2019;64.
19. Sallusto F, Lenig D, Förster R, Lipp M, Lanzavecchia A. Two subsets of memory T lymphocytes with distinct homing potentials and effector functions. Nature 1999;402:34-38.

20. **Lucifora J, Xia Y**, Reisinger F, Zhang K, Stadler D, Cheng X, et al. Specific and nonhepatotoxic degradation of nuclear hepatitis B virus cccDNA. Science 2014;343:1221-1228.

21. Wooddell CI, Yuen M-F, Chan HL-Y, Gish RG, Locarnini SA, Chavez D, et al. RNAi-based treatment of chronically infected patients and chimpanzees reveals that integrated hepatitis B virus DNA is a source of HBsAg. Science translational medicine 2017;9:eaan0241.

22. Velkov S, Ott JJ, Protzer U, Michler T. The Global Hepatitis B Virus Genotype Distribution Approximated from Available Genotyping Data. Genes (Basel) 2018;9.

23. Amann M, Brischwein K, Lutterbuese P, Parr L, Petersen L, Lorenczewski G, et al. Therapeutic window of MuS110, a single-chain antibody construct bispecific for murine EpCAM and murine CD3. Cancer Res 2008;68:143-151.

24. Wu L, Seung E, Xu L, Rao E, Lord DM, Wei RR, et al. Trispecific antibodies enhance the therapeutic efficacy of tumor-directed T cells through T cell receptor co-stimulation. Nature Cancer 2020;1:86-98.

25. Hornig N, Kermer V, Frey K, Diebolder P, Kontermann RE, Muller D. Combination of a bispecific antibody and costimulatory antibody-ligand fusion proteins for targeted cancer immunotherapy. J Immunother 2012;35:418-429.

26. Haagen I-A, de Lau WBM, Bast BJEG, Geerars AJG, Clark MR, de Gast BC. Unprimed CD4+ and CD8+ T cells can be rapidly activated by a CD3×CD19 bispecific antibody to proliferate and become cytotoxic. Cancer Immunology, Immunotherapy 1994;39:391-396.

Figure legends

Figure 1. BsAbs are produced with high purity and bind T-cell antigens specifically.

(A) Schematic representation of FabMAb (i) and BiMAb (ii) formats. **(B)** 2.5 µg of the purified recombinant bispecific antibody was separated by SDS-PAGE under reducing and non-reducing conditions. Coomassie staining of total protein relative to a pre-stained size marker is shown. **(C,D)** Flow cytometry analysis of **(C)** human IgG Fc (BiMAb) and **(D)** His Tag (FabMAb) on $CD4^+$, $CD8^+$ T cells, NK cells, B cells and monocytes after incubation with 10 nM (BiMAbαCD3), 300 nM (BiMAbαCD28), 30 nM (FabMAbαCD3), and 3 µM (FabMAbαCD28) of indicated BiMAb (top) or FabMAb (bottom).

Figure 2. BsAbs bind HBVenv with high affinity. (A) Binding of a dilution series of BiMAb (top) or FabMAb (bottom) to coated, human serum-derived HBsAg determined by ELISA. Mean ± SD of three independent analyses n=9 is shown. EC_{50} values were calculated using non-linear regression log(agonist) vs. response variable slope with a robust fit. **(B)** Binding of BiMAb (left) and FabMAb (right) to HBsAg of different geno- and subtypes by ELISA. Optical density $(OD)_{450}$ is given normalized to the value determined for A1_adw2 (single values). **(C)** Confocal microscopy of Huh7 cells expressing an mCherry-HBVenv fusion protein after incubation with 50 nM of BiMAb (top) or FabMAb (bottom) stained using goat anti-human IgG. Cell membranes are stained with wheat germ agglutinin (WGA). Scale bar is 20 µm.

Fig. 3. HBVenv-directed T-cell engager antibodies induce polyfunctional effector T cells. (A-C) PBMC isolated from healthy subjects were cultured for 72

hours on HBsAg-coated plates in the presence of 3 nM CD3- or CD28-targeting BiMAb or FabMAb, or the combination of CD3- and CD28-binding antibodies (1:1 ratio). **(A)** Exemplary flow cytometry analyses of CD25 expression on $CD8^+$ T cells treated with BiMAb (left) or FabMAb (right). **(B)** Percentage (top) and mean fluorescence intensity (MFI) (bottom) of $CD25^+$ and LAMP-1^+ $CD8^+$ T cells. **(C)** Cell trace violet staining of $CD8^+$ (top) and $CD4^+$ (bottom) T cells. **(D)** IFNγ (top), IL-2 (middle) and TNFα (bottom) determined by ELISA after addition of increasing concentrations of a combination of CD3- and CD28-targeting BiMAb or FabMAb, or without antigen (w/o Ag) or antibody (w/o Ab). **(E,F)** PBMC were co-cultured with Huh7S cells in the presence of CD3- and CD28-targeting (1:1 ratio) BiMAb or FabMAb. **(E)** Concentrations of IFNγ (top), IL-2 (middle), and TNFα (bottom) determined by ELISA in cell culture supernatants at indicated time points after addition of 3 nM bsAbs. Controls are the 72 hour time point without bsAb (w/o Ab) or using HBVenv-negative Huh7 cells (w/o Ag). **(F)** Intracellular staining of IFNγ, IL-2, and TNFα in $CD8^+$ (top) and $CD4^+$ (bottom) T cells at indicated time points to determine polyfunctionality of T cells. Shaded areas indicate cytokine combinations detected. **(G,H)** PBMC were cultured on HBsAg-coated or control plates with 3 nM combination of CD3- and CD28-targeting BiMAb or FabMAb (1:1 ratio) for 72 hours. **(G)** Secreted cytokines were quantified employing Luminex100 machine with BioPlex Manager 6.1 software. Data are presented as fold-change compared to control without antibodies. **(H)** Percentage of naïve ($T_{N,}$ $CD45RA^+CCR7^+$), central memory ($T_{cm,}$ $CD45RA^-CCR7^+$), effector memory ($T_{em,}$ $CD45^-CCR7^-$) and effector memory re-expressing CD45RA T cells ($T_{emra,}$ $CD45RA^+CCR7^-$) was determined after flow cytometry staining of CD45RA and CCR7[19]. Data are presented as mean values of triplicate co-cultures (*n* = 3) (B,D-F) ± SD (B,D,E), or mean values of hexaplicate co-cultures (*n* = 6) (G).

Fig. 4. T-cell engager antibodies activate cytotoxic T-cell function. PBMC were co-cultured with HBVenv-positive Huh7S cells with 3 nM of CD3- and CD28-targeting (1:1 ratio) BiMAb or FabMAb combination. **(A)** Intracellular staining of granzyme B (grzB) in $CD8^+$ (top) and $CD4^+$ (bottom) T cells at indicated time points of co-culture. Controls are the 48 hour time point without antibodies (w/o Ab) or using HBVenv-negative Huh7 cells (w/o Ag). **(B-D)** Huh7 and Huh7S target cell viability was determined over 96 hours after addition of bsAb and PBMC employing an xCELLigence real-time cell analyzer and plotted over time. **(B)** Cell viability after addition of increasing doses of BiMAb (top) or FabMAb (bottom). **(C)** PBMC were depleted of $CD8^+$, $CD4^+$ or both and cultured with Huh7S cells in the presence of BiMAb (top) or FabMAb (bottom). **(D)** $CD8^+$ and $CD4^+$ were isolated and added singly or in combination to Huh7S cells in the presence BiMAb (top) or FabMAb (bottom). Samples without (w/o) PBMC served as controls. **(E)** IFNγ levels in the supernatant after 96 hour co-culture of PBMC depleted from T-cells (top) or sorted T-cell preparations (bottom) with Huh7S cells treated with BiMAb or FabMAb relative to that without (PBMC only). **(F)** xCELLigence analysis of PBMC from 4 different healthy donors (D1-D4) and from a chronically infected hepatitis B patient (CHB). **(G)** HBVenv-transgenic HepG2 660 and HepG2 were mixed as indicated and co-cultured with PBMC and 10 nM BiMAb (top) or FabMAb (bottom). **(H)** Correlation between IFNγ in the supernatant and percent of Huh7S cells after 72 hour co-culture of PBMC with indicated mixtures of Huh7S cells and Huh7 cells with BiMAb (top) or FabMAb (bottom). Data are presented as mean values ± SD of triplicate (n = 3) (A-G), or hexaplicate (n = 6) co-cultures (H).

Fig. 5. T-cell engager antibodies allow redirection of T cells towards HBV-infected hepatocytes and trigger target cell elimination. HepG2-NTCP cells were infected with HBV at indicated MOI. **(A)** Percentage of HBV core-positive ($^+$) HepG2-NTCP cells 8 days after mock infection (left) or infection at MOI 500 virions/cell (right) determined by flow cytometry. **(B)** Flow cytometry analysis of HepG2-NTCP cells infected at MOI 500 virions/cell after incubation with either anti-CD3 or anti-CD28 BiMAb and staining with anti-human IgG. **(C,D)** 8 days post infection at increasing MOIs of HBV, PBMC and a 1:1-combination of anti-CD3 and anti-CD28 FabMAb were added at indicated concentrations. **(C)** IFNγ, IL-2 and TNFα were measured by ELISA in supernatants of co-cultures after 72 hours. **(D)** Viability of HBV-infected cells was monitored over 96 hours employing an xCELLigence real-time cell analyzer. Controls were without antibodies (w/o Ab) or non-infected HepG2-NTCP cells (HBV neg). Data are presented as mean values ± SD of triplicate co-cultures (*n* = 3).

Fig. 6. T cells redirected by bsAbs show antiviral effector function. (A-D) HepG2-NTCP cells were infected with HBV at MOI 500 virions/cell and co-cultured with PBMC in the presence of a 1:1-combination of anti-CD3 and anti-CD28 BiMAb or FabMAb from day 8 post infection. **(A)** BiMAb (left) or FabMAb (right) were added at indicated concentrations. HBeAg in cell culture supernatants was determined at indicated time points. **(B)** Representative Southern blot analysis of intracellular HBV-DNA after 12-day co-culture with PBMC and 10 nM BiMAb or FabMAb or without antibodies (w/o Ab). HBV relaxed circular DNA (rcDNA) and replication intermediates are indicated. **(C)** Levels of HBeAg secreted from day 10-12 (top), intracellular total HBV-DNA (middle) and HBV cccDNA (bottom) after 12-day treatment with 10 nM BiMAb or FabMAb relative to cultures without antibodies (w/o Ab). **(D)** HBeAg-values

secreted from day 10-12 (top), intracellular total HBV-DNA (middle) and HBV cccDNA (bottom) after 12-day treatment with BiMAb or FabMAb using half-logarithmic dilution from 100-0.03 nM. IC_{50} was calculated by non-linear regression log(inhibitor) vs. normalized response analysis - variable slope with a robust fit. **(E)** HepG2-NTCP cells were infected with HBV at indicated MOI, co-cultured with PBMC in the presence of FabMAb at indicated concentrations for 12 days. HBeAg secreted from day 10-12 (top), intracellular total HBV-DNA (middle) and HBV cccDNA (bottom) were determined relative to control infected at MOI 500 virions/cell but no antibody added. **(F)** To determine the indirect, non-cytolytic antiviral effect of T-cell stimulation, PBMC and HBV-infected target cells were separated using a transwell system. HBV-infected HepaRG cells and a transwell containing Huh7S cells, PBMC and 3 nM BiMAb combination as indicated were cultured for seven days. Levels of total intracellular HBV-DNA (left) and HBV cccDNA (middle) in infected HepaRG cells determined by qPCR relative to the cellular prion protein (PRP) gene, and levels of HBeAg secreted from day 0-7 (right) are shown. Data are presented as mean values ± SD of triplicate cocultures (*n* = 3). To calculate p-values, we employed two-tailed unpaired t-tests. nd=not detectable.

Fig. 7. BiMAb target HBVenv-expressing hepatocytes *in vivo*. C57BL/6 mice (n=3 per group) were injected with 50 µg of **(A)** BiMAbαCD28 or **(B)** FabMAαCD28 in 200 µl PBS either i.v., i.p. or s.c.. Control mice were injected with 200 µl PBS i.v.. Alternating groups of mice were bled after 1, 6, 12, 24, 48 and 72 hours, and antibody concentrations in serum were determined using the Architect® anti-HBs assay (BiMAb) or ELISA (FabMAb). Anti-HBs levels are given relative to the 1 hour time point of the i.v. injected group (set to 100%). BiMAb data is given as mean ± SD of single analyses for each mouse (n=3). FabMAb data represent mean ± SD of

technical duplicates for each mouse (n=6). **(C,D)** Immunohistochemistry staining for human IgG in livers of **(C)** HBV1.3xfs and **(D)** HBV-naïve C57BL/6 mice collected 2 hours after i.v. injection of 50 µg and 100 µg of BiMAbαCD3 or BiMAbαCD28. Control animals received PBS. Scale bar is 100 µm.

Fig. 8. BiMAb control HBVenv-expressing tumors *in vivo*. (A) Schematic representation of the *in vivo* experimental analysis of BiMAb in Rag2/IL2Ryc$^{-/-}$ mice. On day 0, 2x10^{6} Huh7 or Huh7S cells were injected subcutaneously into the left and the right flank of each animal, respectively. On day 14, mice were i.p. injected with 2x10^{7} human PBMC and i.v. injected with a combination of 100 µg BiMAbαCD3 and 100 µg BiMAbαCD28 (n=14) or PBS (n=14). Application of antibodies was repeated three times every two days. Mice were sacrificed on day 23, and tumors and sera were collected**. (B)** Size of HBVenv-negative (Huh7, left panel) and HBVenv-positive (Huh7S, right panel) tumors after 10-day treatment with or without BiMAb. **(C,D)** Fold increase of human (h)CD4 (left) and hCD8 (right) mRNA in **(C)** HBVenv-positive tumors and **(D)** HBVenv-negative tumors after 10-day treatment with BiMAb. mRNA levels of hCD4 and hCD8 were determined by qPCR and normalized to GAPDH. Note that only detectable tumors could be analyzed, and samples without detectable GAPDH mRNA were excluded. **(E)** HBsAg levels in mouse sera after 10-day treatment with BiMAb were quantified using the Architect quantitative HBsAg® assay. Data represent mean ± SD. p-values were calculated using Mann-Withney u test.

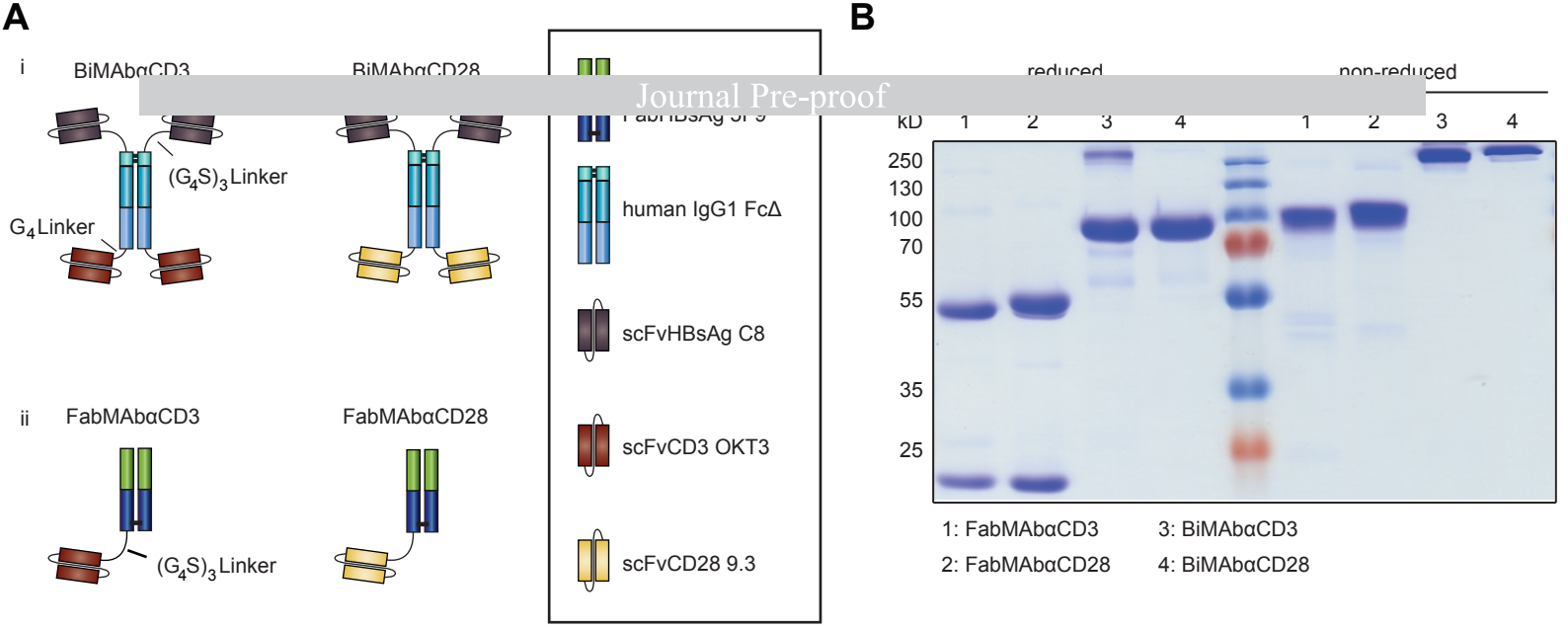

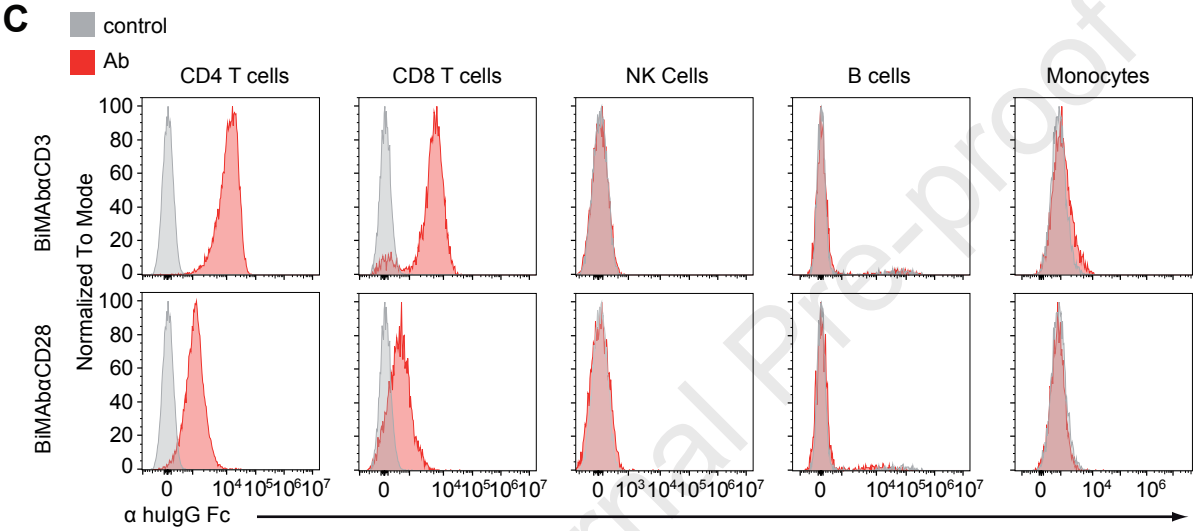

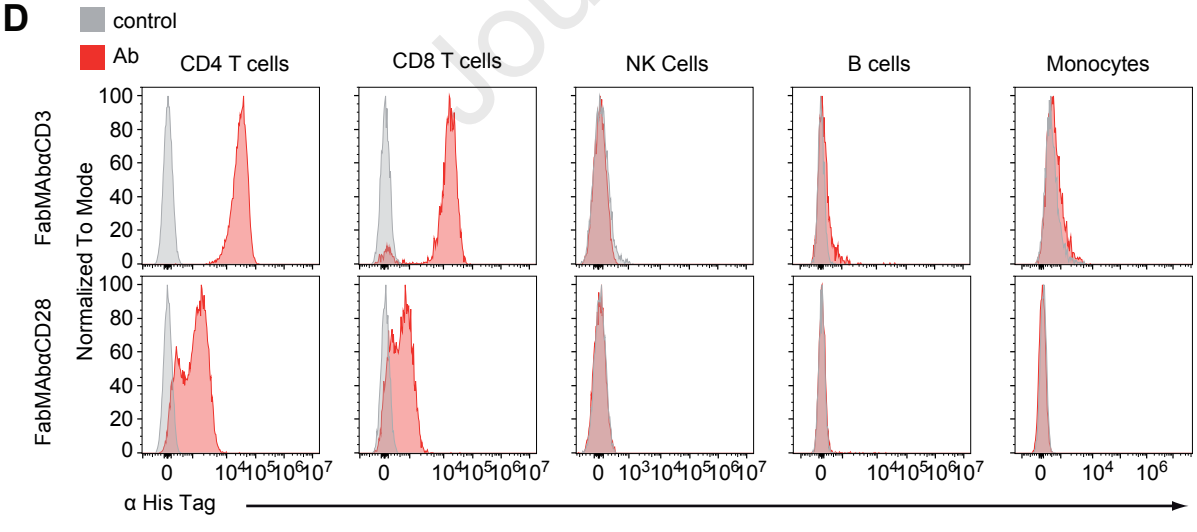

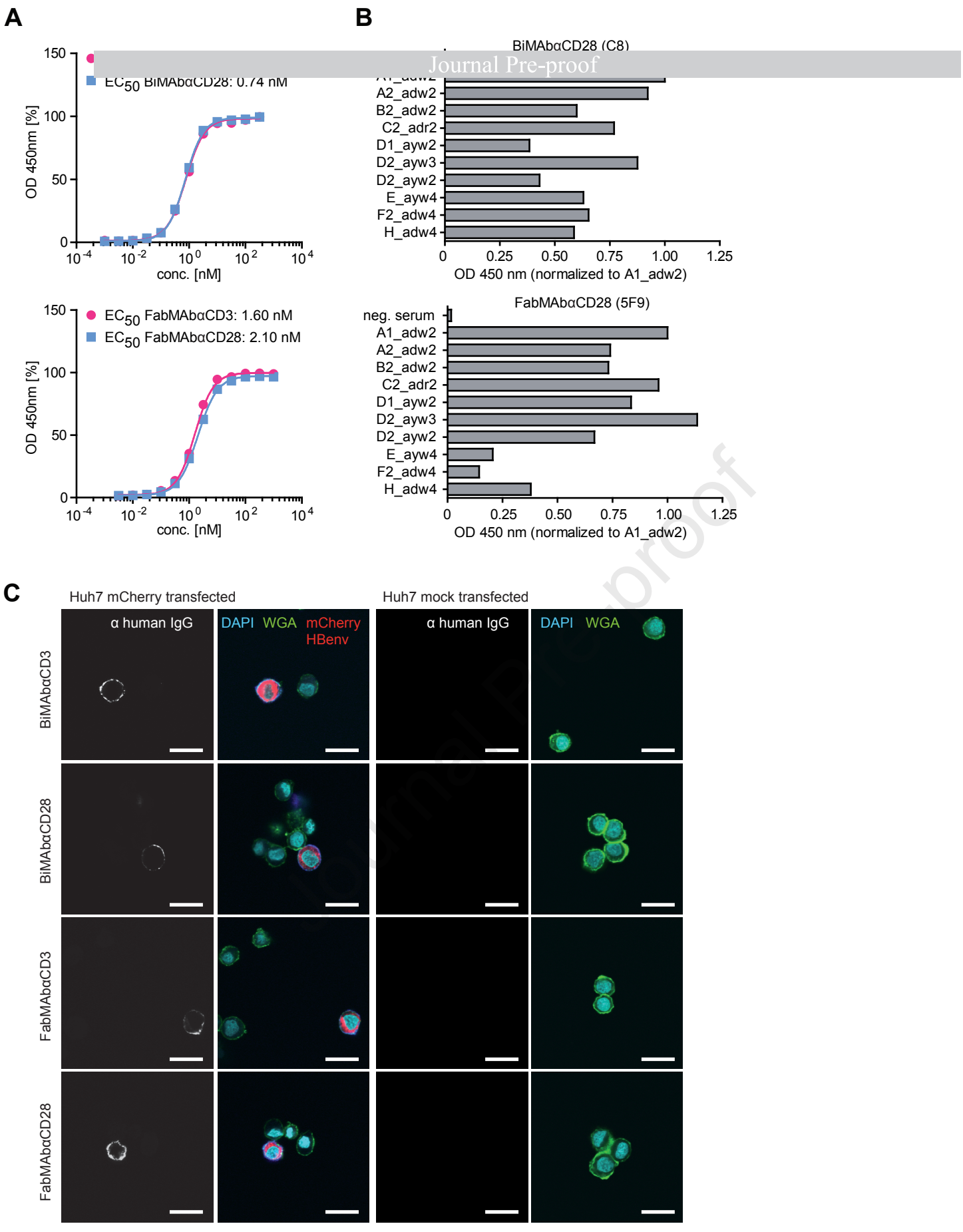

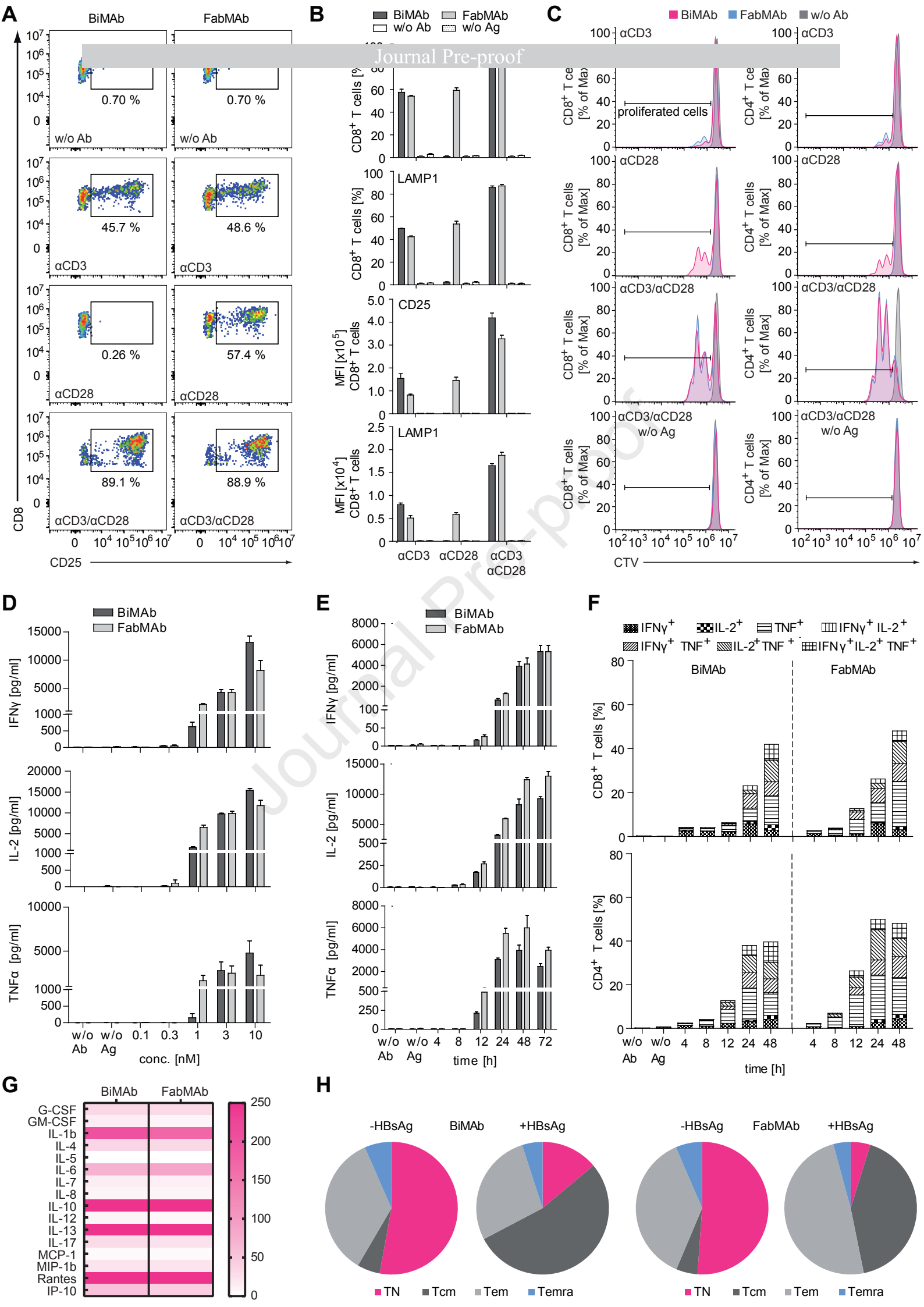

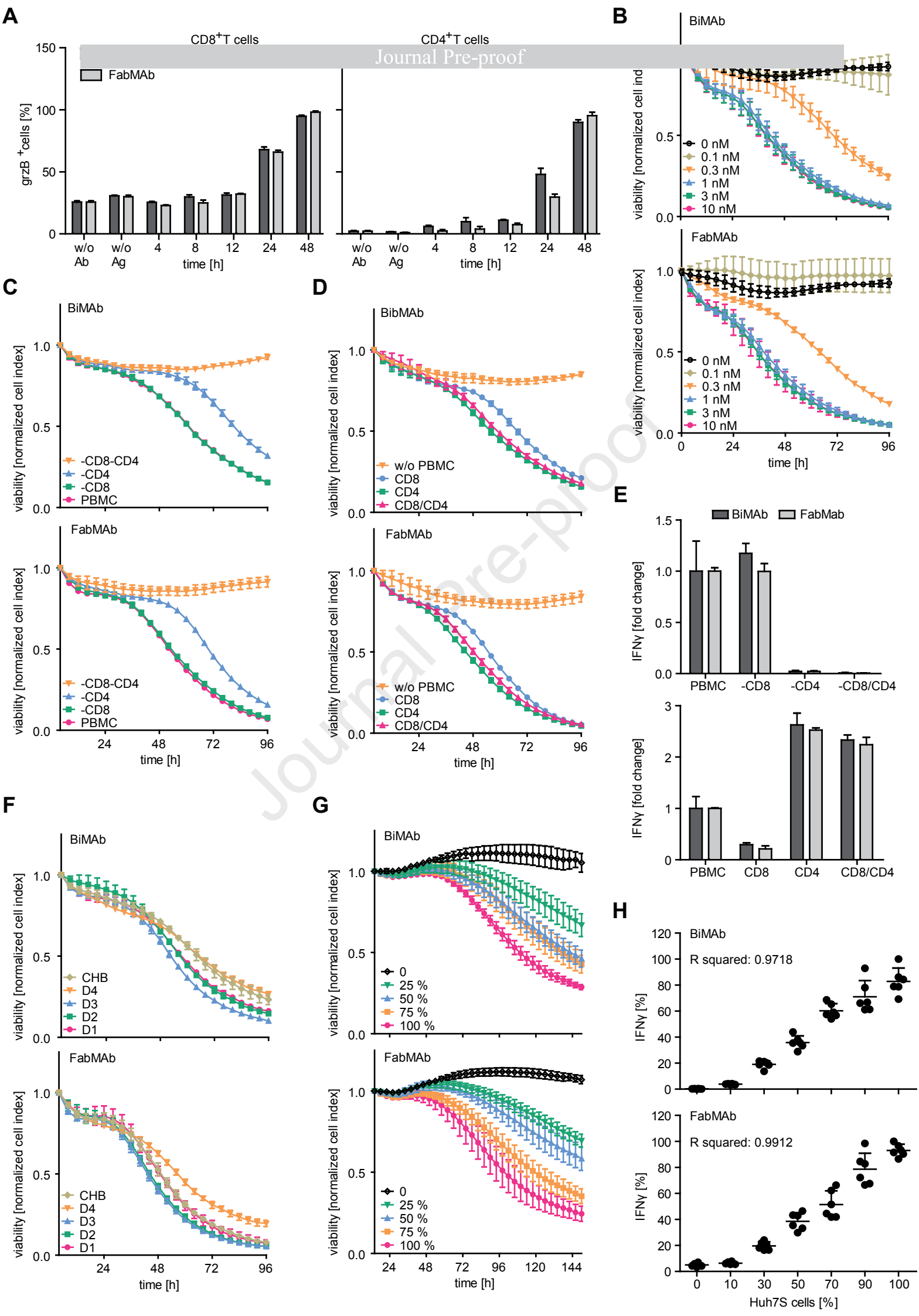

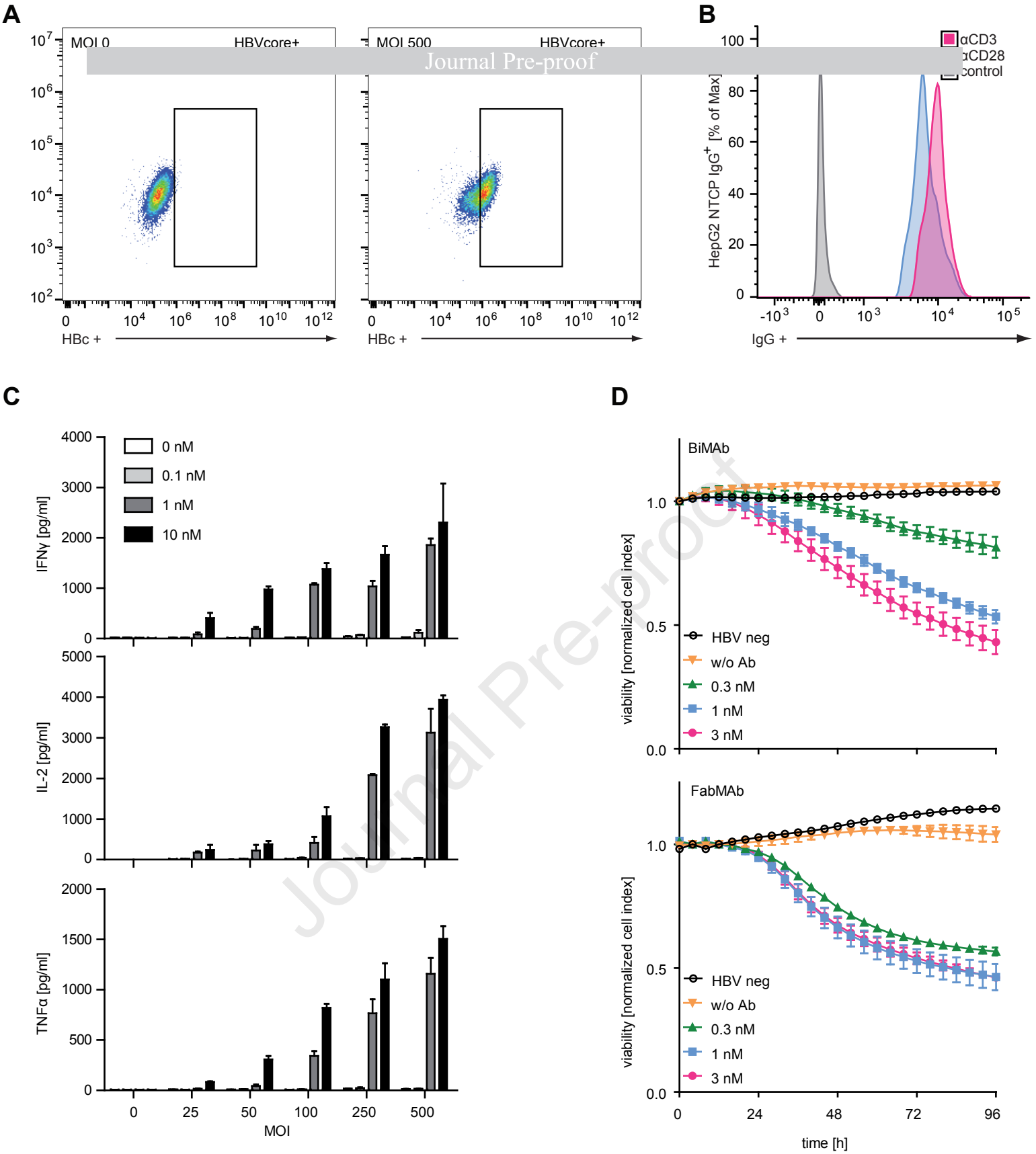

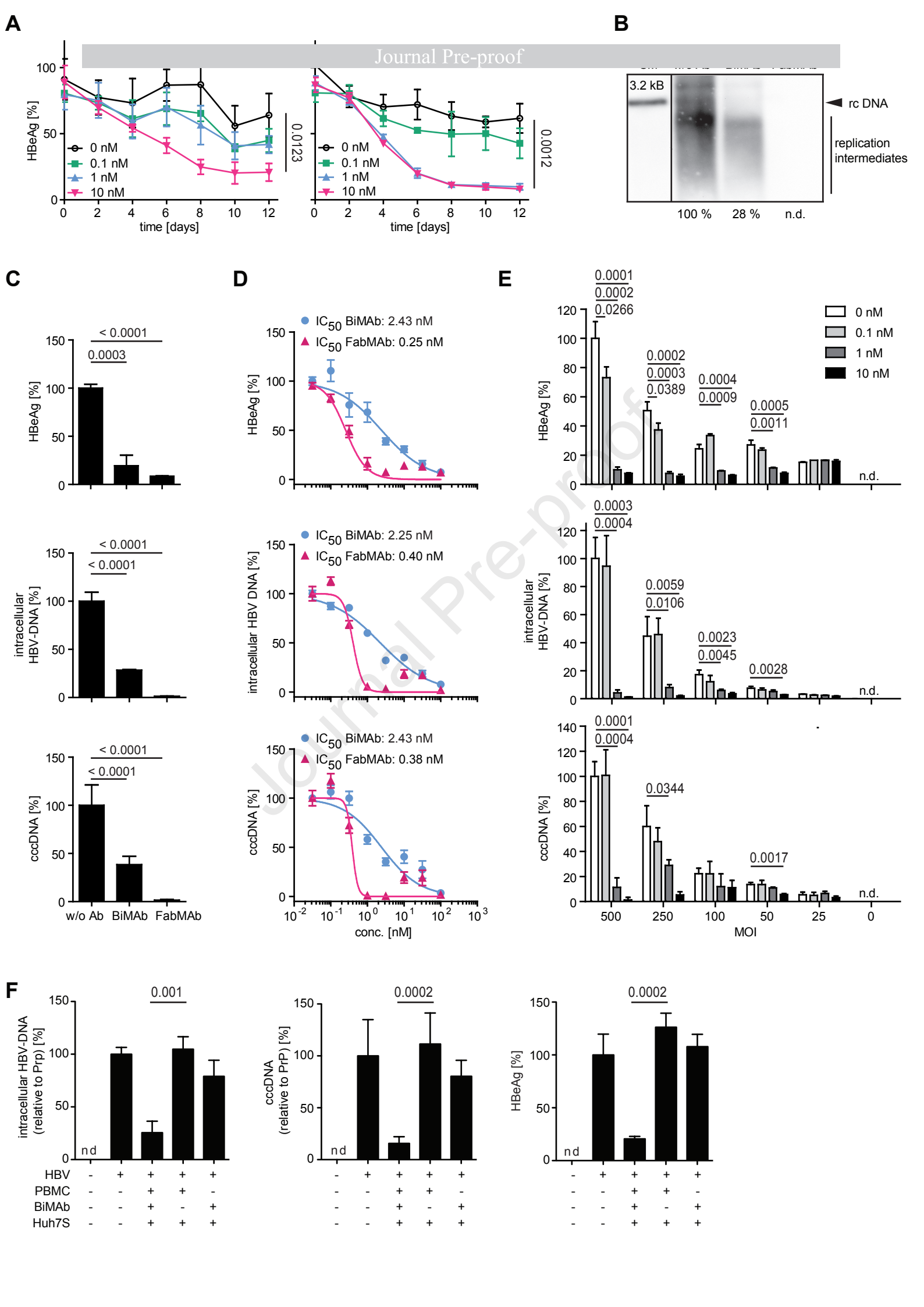

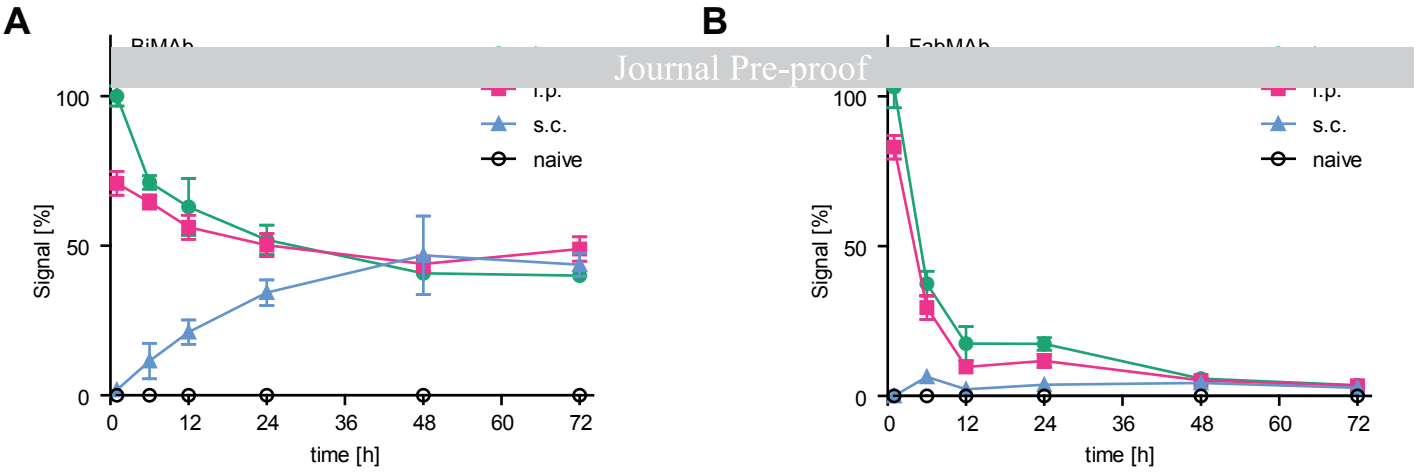

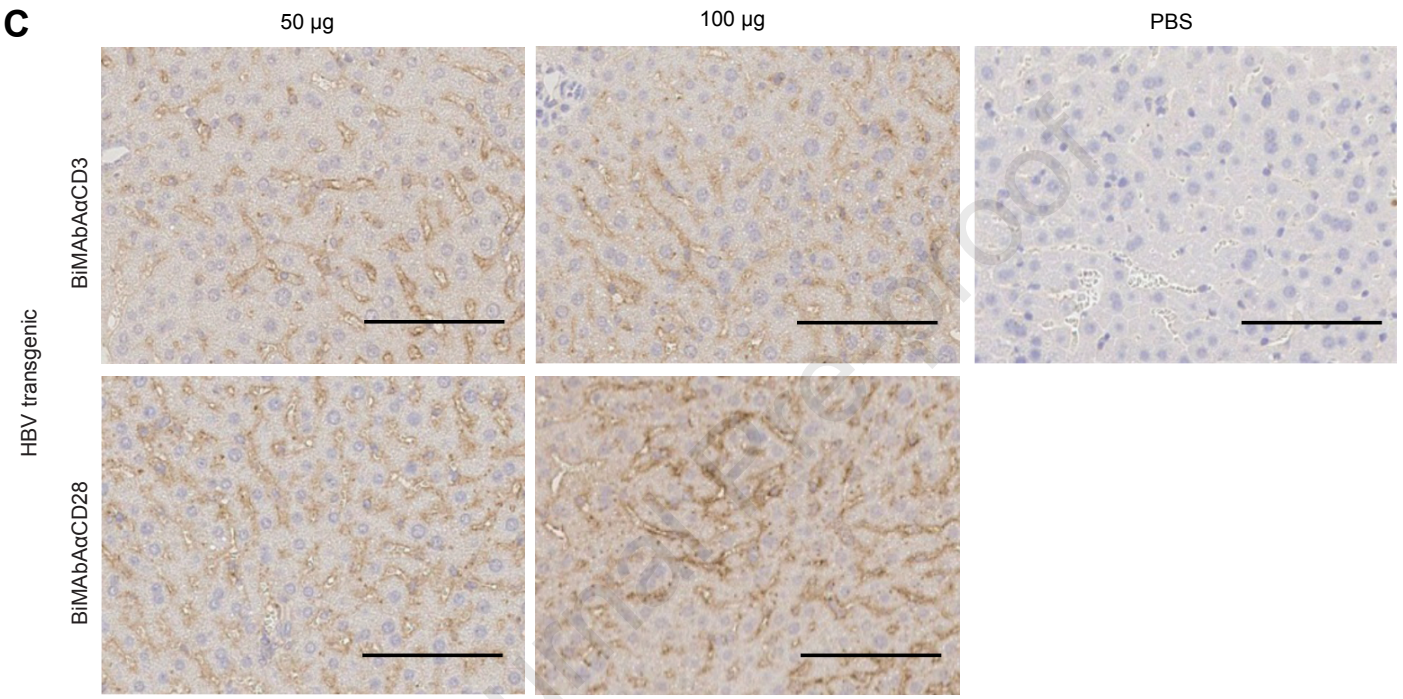

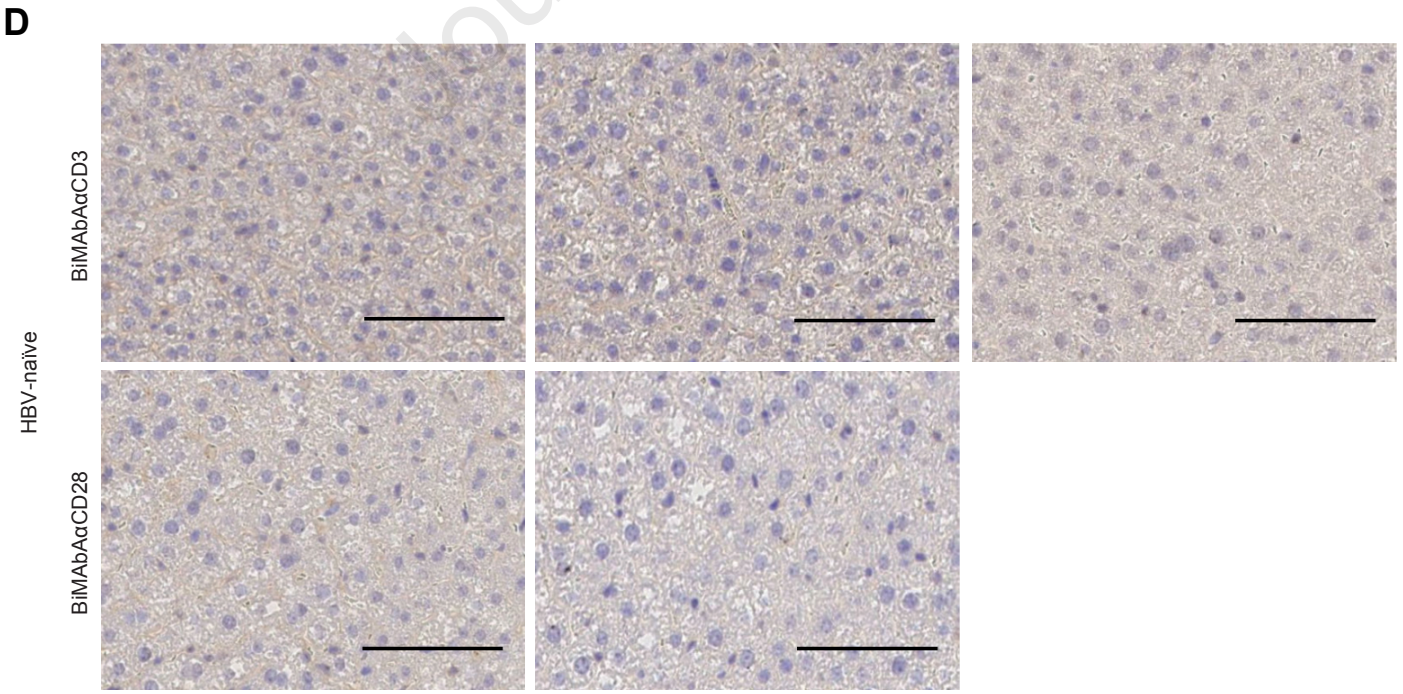

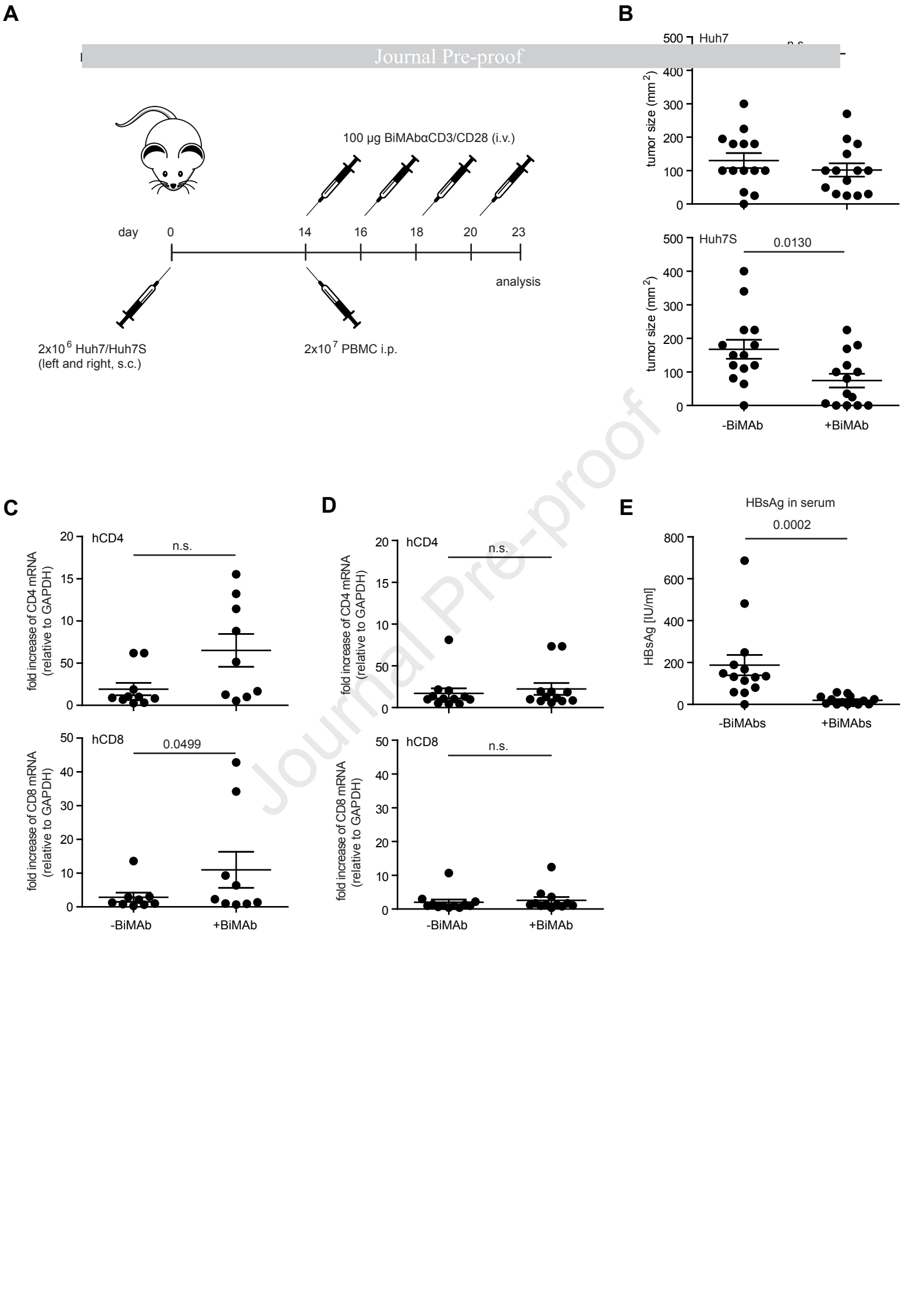

Highlights:

- HBV cure most likely requires reconstitution of anti-HBV immunity
- T-cell engager antibodies direct and activate T cells on a desired target
- We designed T cell engagers that bind HBV envelope proteins and CD3/CD28 on T cells
- HBV-specific T cell engagers activate T cells and stimulate their antiviral activity
- Engaged T cells control HBV replication and eliminate HBV-positive hepatoma *in vivo*